Variation of LDF during a sea period

Rodolfo Avila, Facilia AB

1. Introduction

This Memo provides a response to question 2 in SSM's request for additional information regarding radionuclide transport and dose (SSM reference no SSM2011-2426-92).

Section 2 provides an explanation for the relative fast changes of LDF for Ra-226 shown in Figure 5-1 (Avila et al. 2010) and Section 3 gives an explanation for the fast changes of activity concentration of Ra-226 and I-129 in surface water shown in Figure 3-5 (Avila et al. 2010). Both these issues are explicitly mentioned in SSM's request.

2. Explanations for the relative fast changes of LDF for Ra-226.

This part of the SSM question refers to Figure 5-1 in Avila et al. (2010) shown below:

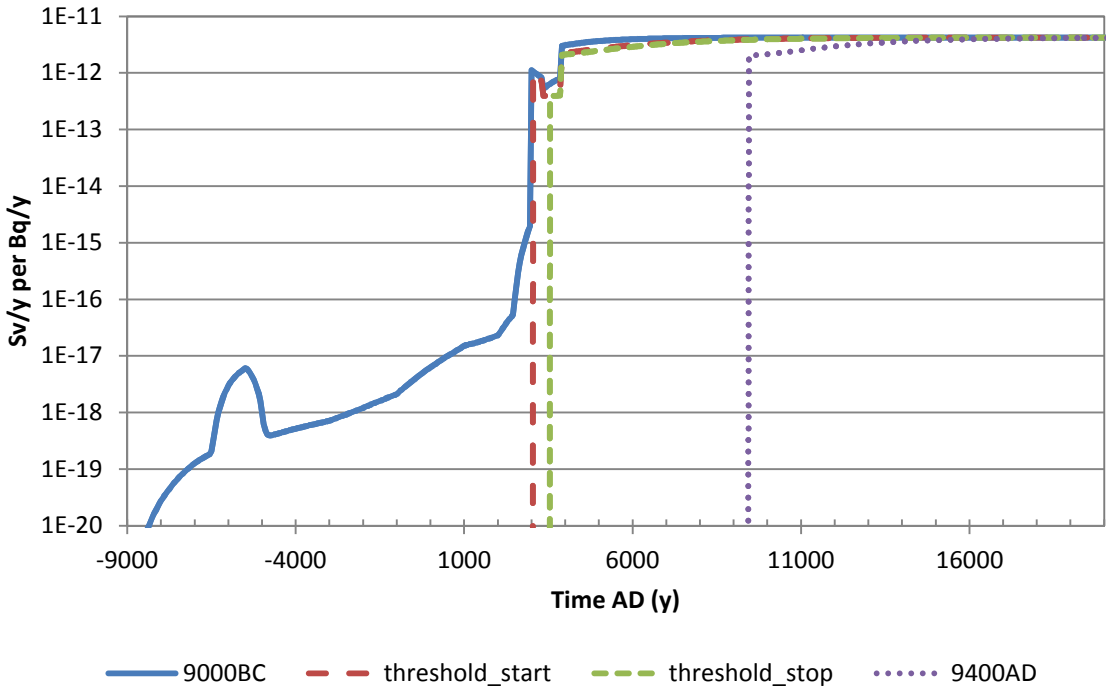

Figure 5-1 in Avila et al. (2010). Time series of annual doses per unit release rate obtained from simulations where 1 Bq/y of Ra-226 is released to the biosphere object with the highest LDF (see Table 4-1). Results are presented for four cases with different starting times of the releases; from the start of the submerged period at 9000 BC (used for the derivation of baseline LDFs), after the end of the submerged period (threshold_start), after the end of the transitional stage (threshold_stop) and after the end of the temperate period at 9400 AD.

Figure 5-1 above was included in Chapter 5 of Avila et al. (2010), which is dedicated to the uncertainty analysis of the LDF values. As explained in Section 5.1.1, page 43 (Avila et al. 2010) this figure is used to illustrate the effect on the LDFs of how timing and duration of the

releases is handled in their derivation. This figure shows that for Ra-226 the timing and duration of the release has no effect on the LDF value, taken as the maximum over the whole simulation period.

SSM request for an explanation of the relative fast changes of LDF values for Ra-226 refers to the blue line in Figure 5-1, which corresponds to the case when there is a constant unit release of Ra-226 during the whole simulation period. It is clear from inspection of Figure 5-1 that fast changes occur only during the Sea Period, i.e. from year 9000 BC until the time when the transformation from Sea to Land starts (time corresponding to threshold start in Figure 5-1). Hence, we will focus our discussion below on the Sea period, which for the specific biosphere object in Figure 5-1 (121-03) extends from 9000 BC to 3000 AD.

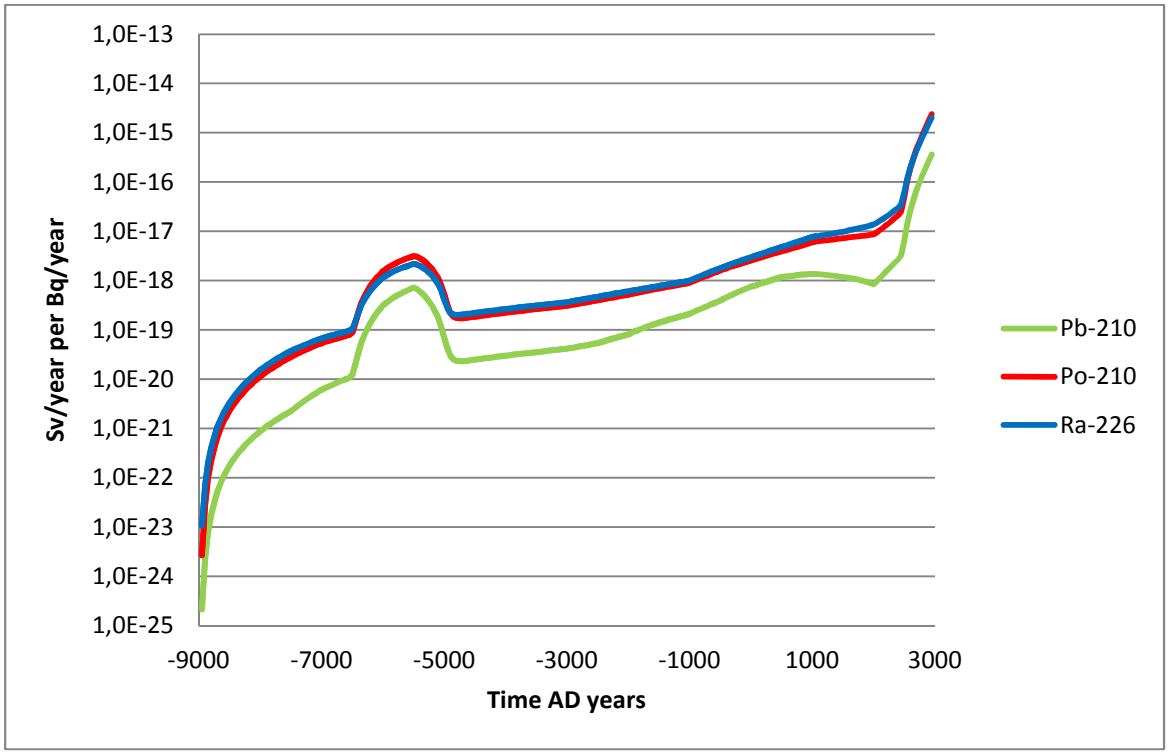

Figure 1. Total doses during the Sea Period obtained from simulations with a constant unit release rate of Ra-226 during the whole period. Values are presented for object 121-03.

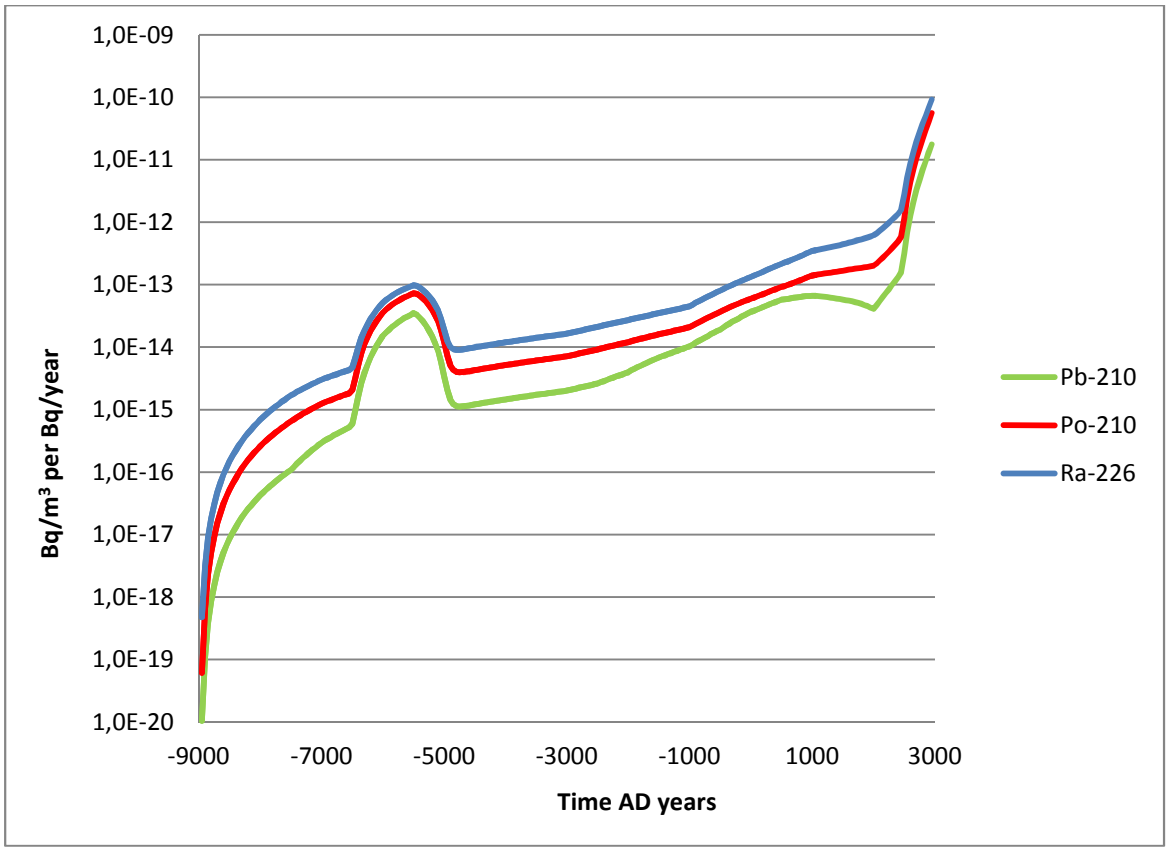

Figure 2. Total activity concentrations in water during the Sea Period obtained from simulations with a constant unit release rate of Ra-226 during the whole period. Values are presented for object 121-03.

The doses during the Sea Period are shown in Figure 1 for Ra-226 and for the two daughter radionuclides (Pb-210 and Po-210) that contribute to the LDF of Ra-226. During the Sea Period the only pathway contributing to the doses is fish ingestion. The doses from fish ingestion (Sv/year) are calculated by multiplying the activity concentration in fish (Bq/kgC) by the ingestion rate of fish (kgC/year) and the dose coefficient for ingestion (Sv/Bq). Both the ingestion rate of fish and the dose coefficient for ingestion are kept constant during the whole simulation period and therefore the calculated doses are proportional the activity concentrations in fish. Hence, the time variation of the calculated doses will always resemble the time variation of the calculated activity concentrations in fish. At the same time, the activity concentrations in fish are proportional to the activity concentrations of the radionuclide dissolved in water, since a constant in time Concentration Ratio (CR) is used for calculating the concentrations in fish from the activity concentrations of the radionuclide dissolved in water. Furthermore, the activity concentrations of the radionuclide in dissolved water is related to the total activity concentrations in water through the Kd for suspended particles and the concentration of suspended particles in water. Both these parameters are kept constant during the entire Sea Period. From the above, it can be expected that during the Sea Period the time dynamics of the doses will resemble the time dynamics of the total activity concentrations in water. This can be confirmed by comparing the time dynamic of the doses in Figure 1 with the time dynamics of the total activity concentrations in water presented in Figure 2.

It can be concluded that the relative fast changes of the LDF for Ra-226 observed in the Sea Period are a result of relative fast changes of the activity concentrations in water. The

reasons for the fast changes of the activity concentrations in water during the Sea Period are discussed in the next Section.

3. Explanations for fast changes of Ra-226 and I-129 activity concentrations in surface water

This part of the SSM question refers to Figure 3-5 in (TR-10-06) shown below:

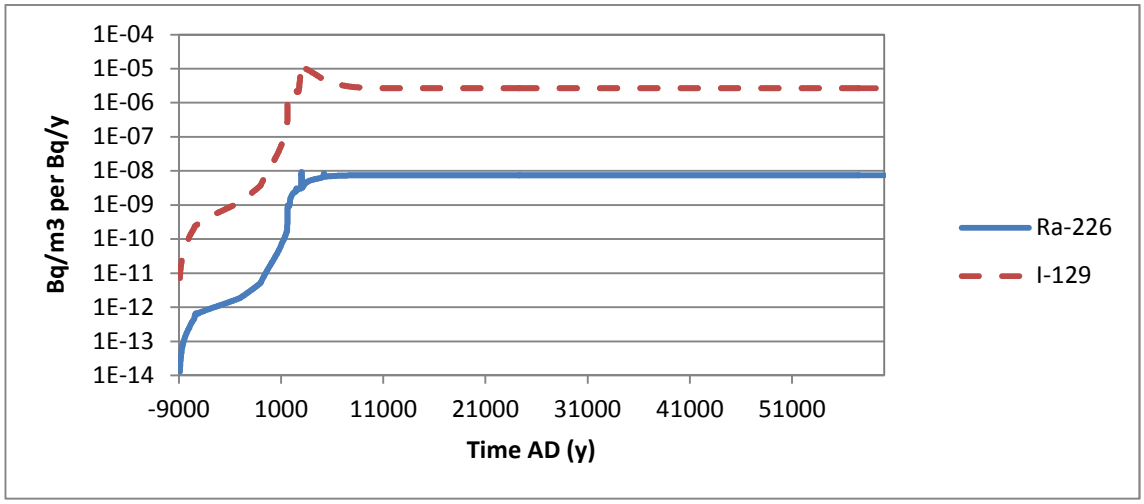

Figure 3-5 in Avila et al. (2010). Activity concentrations of Ra-226 and I-129 in surface waters. Maximum values across all biosphere objects are shown. The values were obtained from deterministic simulations with a constant unit release rate during the interglacial period.

Figure 3-5 above is included in Section 3.5 (Avila et al. 2010), which is dedicated to the description of simulations that were carried out for derivation of LDF values. The intention with this figure is merely to illustrate the type of intermediate results that are generated during the derivation of LDF values, in this case the concentrations in surface waters, and their time trends and levels. The figure shows the maximum value across all biosphere objects at each time step. The maximum values at different time steps might be obtained in different biosphere objects, which is the case here. This explains, for example, the two spikes that can be seen after year 1000 AD in the curve for Ra-226. (The spikes are hence not due to instabilities of the numerical integration, but a direct effect of the dynamics of the model.)

From Figure 3-5 it is seen that fast changes in the activity concentrations in surface waters occur only during the Sea Period and therefore our discussions below will be focus on this period. Further, we will use the time series of activity concentrations in surface water (Sea water) obtained for one specific object (object 121-03), which are shown for Ra-226 and I-129 in Figure 3. This is more suitable for explaining time variations than using maximum values across all biosphere objects. It should be noted that the obtained time dynamics of activity concentrations in surface waters was very similar for all biosphere objects.

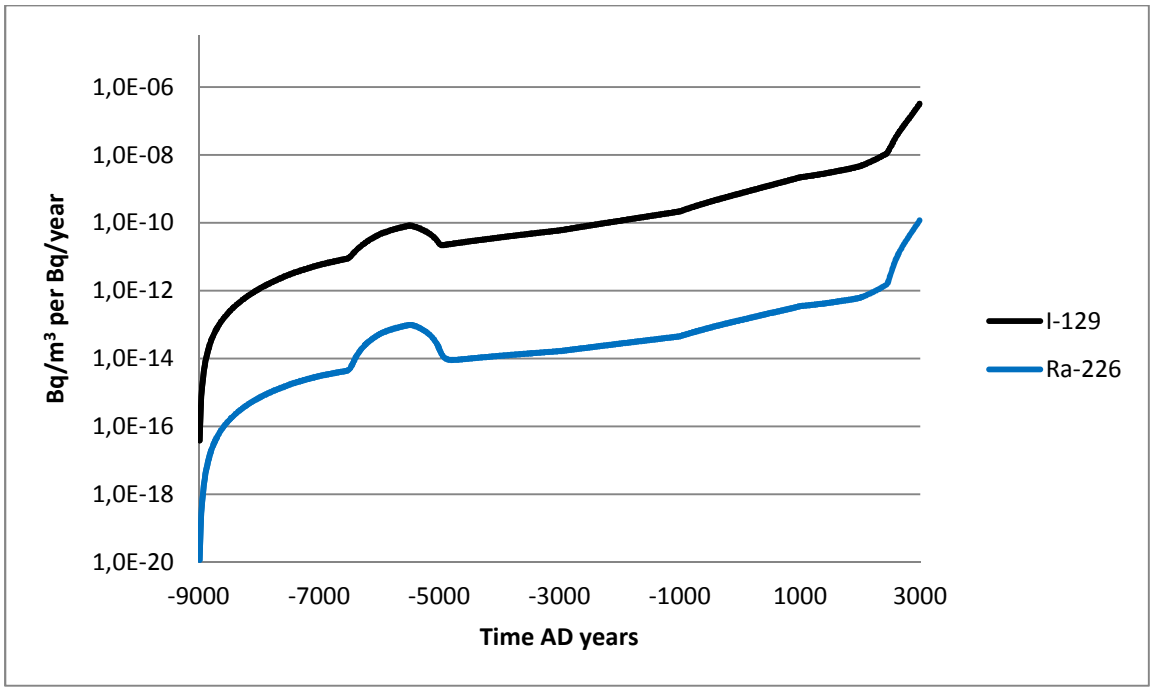

Figure 3. Total activity concentrations of Ra-226 and I-129 in water during the Sea Period obtained from simulations with a constant unit release rate of these radionuclides during the whole period. Values are presented for object 121-03.

Both for Ra-226 and I-129 several orders of magnitude increase of the activity concentrations in water during the Sea Period is observed (Figure 3). The time series of the activity concentration in water look very similar for these two radionuclides and this is also the case for all other radionuclides considered in SR-Site. The activity concentrations in water are obtained for each time step with a compartment model, by dividing the inventory in the water compartment with the volume of the compartment. In practice this is the same as dividing the radionuclide flux from the compartment (Figure 4) with the water flux from the compartment (Figure 5).

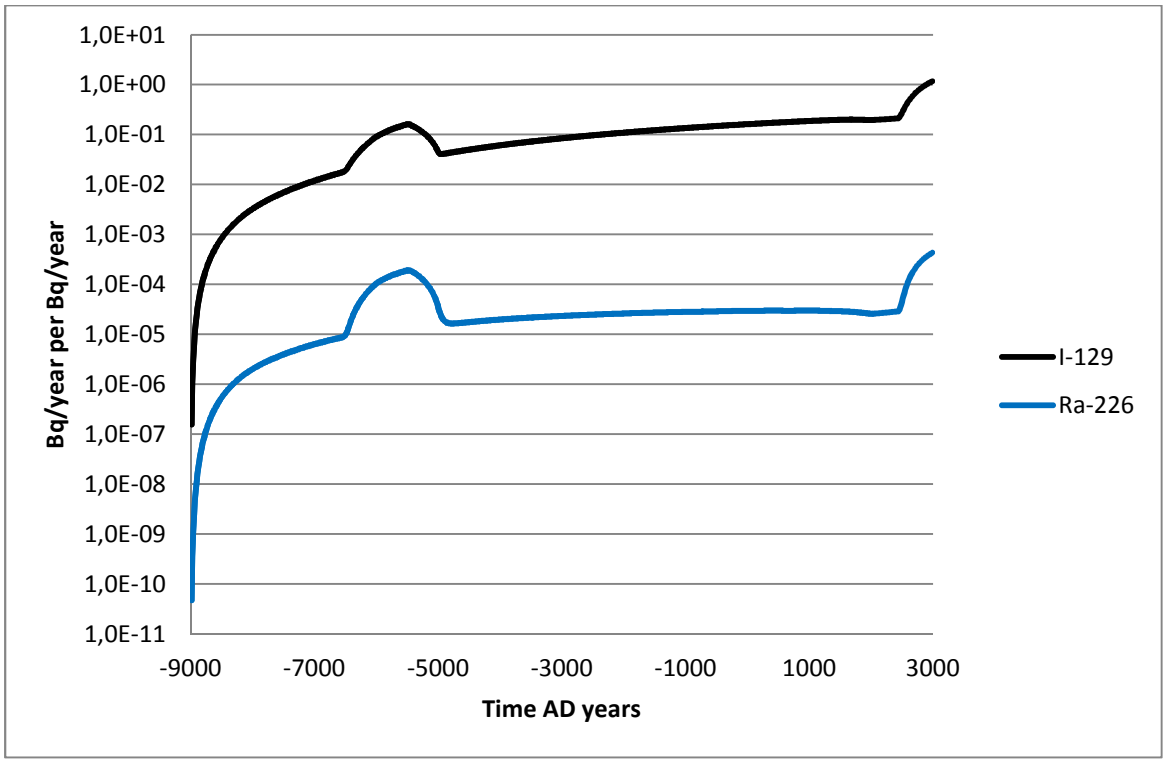

Figure 4. Flux of Ra-226 and I-129 from the biosphere object during the Sea Period obtained from simulations with a constant unit release rate of these radionuclides during the whole period. Values presented for object 121-03.

The fluxes of Ra-226 and I-129 from the compartment increase with time towards a steady state value, which is, as expected, close to 1 for I-129 that has a very long half life and is lower for Ra-226 because of its relatively short half life. The deviation from monotonicity that is observed in the time period around 7000 BC to 5000 BD and the sudden increase at the end of the Sea Period are due to resuspension of sediments and will be discussed later on. If such resuspension processes had been disregarded and the water fluxes from the object were kept constant, then an exponential monotonic increase towards the steady state value would have been obtained from the simulations. The lower the retardation in the regolith the faster would be the increase of the fluxes and the earlier steady state would be achieved. The retardation in the regolith depends on the Kd (the higher the Kd the higher the retardation), which is different for different radionuclides. From comparison of the curves in Figures 3 and 4 it is clear that the increase in time of activity concentrations in water is faster than the increase of radionuclide fluxes from the object. Hence, a factor or several, other than retardation in the regolith should be at play. As it will be shown below, such a factor is the rapid decrease of the water fluxes from the biosphere object (see Figure 5) that is assumed in the model.

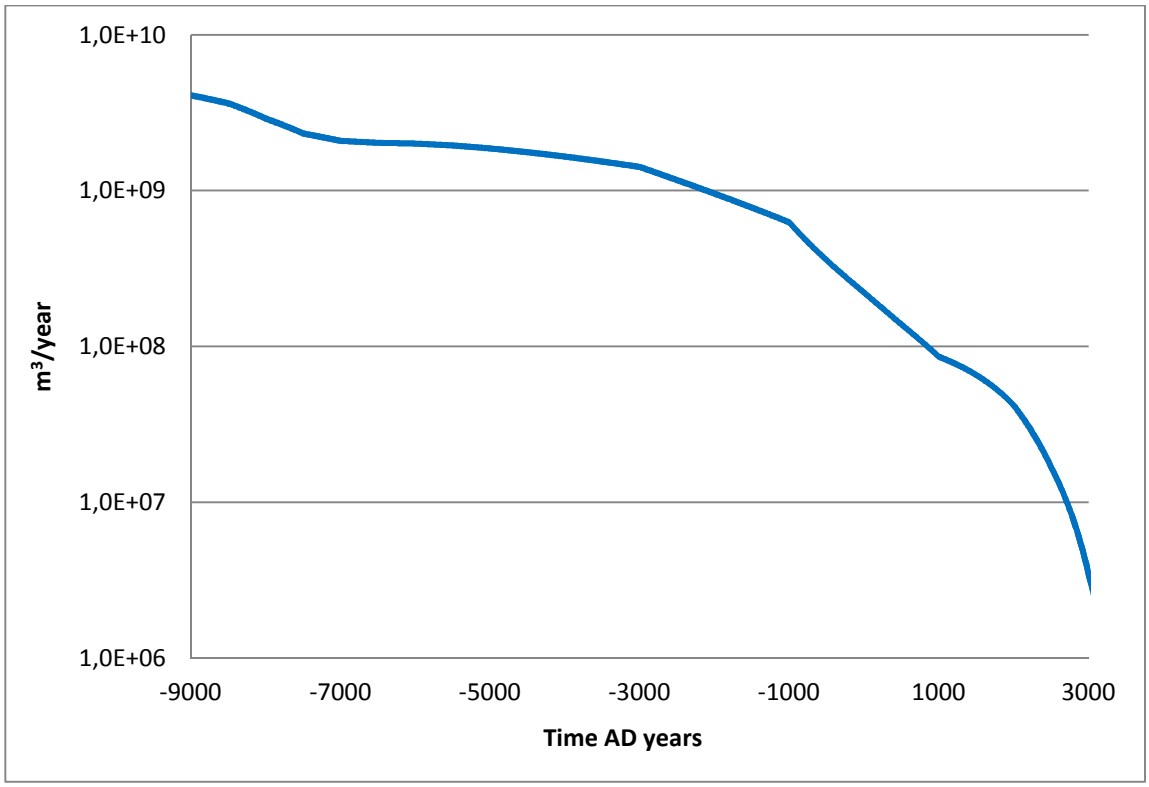

Figure 5. Flux of water from the biosphere object during the Sea Period. Values presented for object 121-03.

Figure 5 shows the time variation of the water flux from the biosphere object (121-03) that is used in the model. It can be seen that the water flux decreases drastically during the simulation period. The speed of the decrease varies during the period, which is reflected in the time dynamics of the activity concentrations in water (Figure 3).

The water fluxes are calculated in the model using three parameters: the area of the biosphere object, the average water depth in the object and the retention time of water in the object. The water retention time experiences moderate variation during the simulation period, whereas changes in depth and area are more drastic. This has to do with the way the model is set up: the releases are first distributed in the whole corresponding Sea Basin and the area and water depth of the object decrease in time due to the shoreline displacement.

In conclusion, the increasing trend of the radionuclide activity concentrations in water is explained from increases of the radionuclide fluxes in and from the water compartment, towards a steady state value and a decrease of the water fluxes through the object; due to the fact that releases are directed to an increasingly smaller and shallower biosphere object, reflecting the shoreline displacement.

The peaks in the water concentrations observed in the time period around 7000 BC to 5000 BC and at the end of the Sea Period are due to resuspension of sediments during these periods. This can be seen from Figure 6, which shows that radionuclide fluxes from the sediments to the water driven by resuspension occur in these periods. The enhanced resuspension caused by the action of sea waves on the bottom sediments, which is predicted at 7000 BC to 5000 BC, when the water depth is sufficiently shallow (ca 30 m) that the sediments can be eroded and the fetch is sufficiently large (ca. 500km) to allow waves with sufficient height to provide high erosion force at these depths. Later emerging islands

and shallows reduces the fetch and power for erosion events until the sediments are close to the shoreline, which causes the resuspension at the end of the sea period (around 3000 AD in figure 3). The modeling of the resuspension events is described in detail by Brydsten (2009) and the resulting dynamics of resuspension events, shoreline displacement and lake isolation in Brydsten and Strömgren (2010).

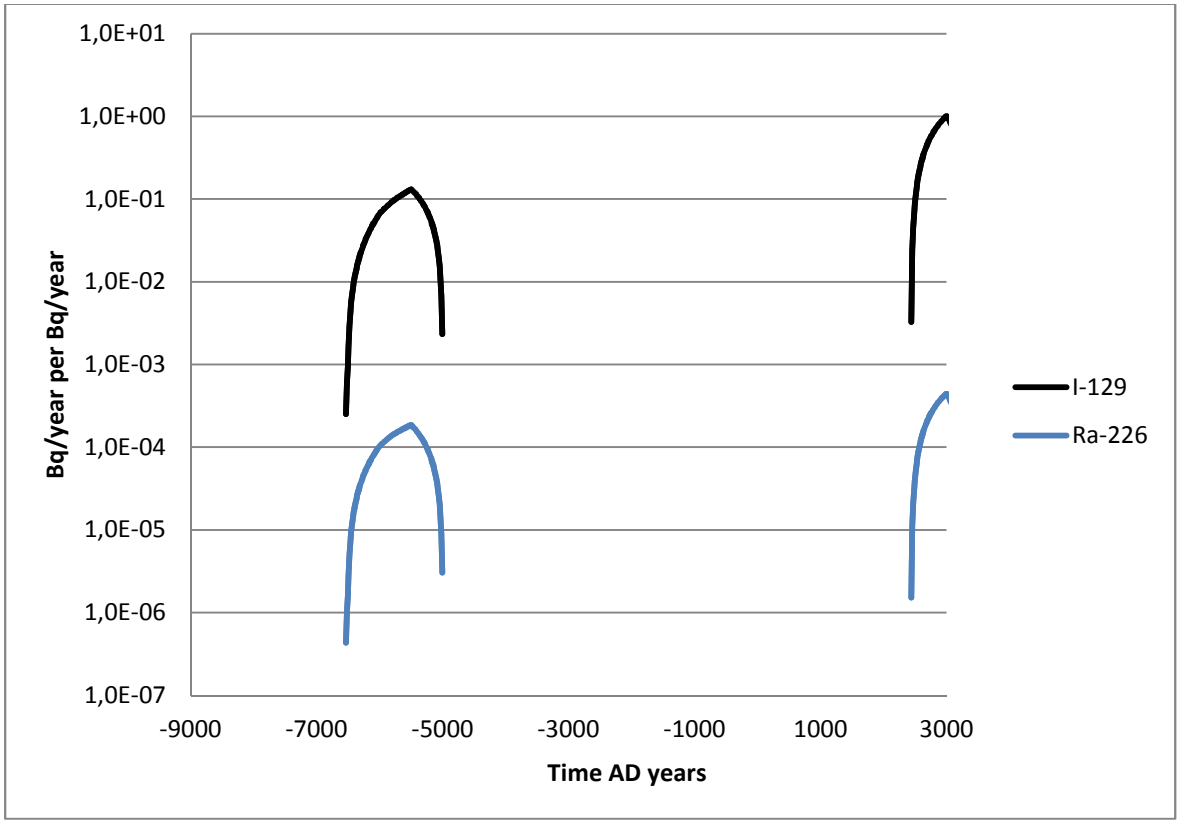

Figure 6. Fluxes of Ra-226 and I-129 from sediment to water driving by resuspension obtained from simulations with a constant unit release rate of these radionuclides during the whole period. Values presented for object 121-03.

References

Avila R, Ekström P-A, Åstrand P-G, 2010. Landscape dose conversion factors used in the safety assessment SR-Site. SKB TR-10-06, Svensk Kärnbränslehantering AB.

Brydsten L, 2009. Sediment dynamics in the coastal areas of Forsmark and Laxemar during an interglacial. SKB TR-09-07, Svensk Kärnbränslehantering AB.

Brydsten L, Strömgren M, 2010. A coupled regolith-lake development model applied to the Forsmark site. SKB TR-10-56, Svensk Kärnbränslehantering AB.